This article has been accepted for publication in IEEE Transactions on Computational Social Systems. This is the author's version which has not been fully edited and content may change prior to final publication. Citation information: DOI 10.1109/TCSS.2025.3599080

LACL: LLM-Augmented Contrastive Learning for Misinformation Detection in Social Networks

Hang Shen, *Member, IEEE,* Xiang Li, Xu Wang, Yuanfei Dai, Tianjing Wang, *Member, IEEE,* and Guangwei Bai

***Abstract*—Misinformation detection in social networks faces challenges due to complex semantics, scarcity of labeled data, and rapidly evolving false narratives. To address these issues, we present LACL (LLM-Augmented Contrastive Learning), a novel framework that integrates large language models (LLMs) with contrastive learning (CL) for robust and accurate misinformation detection. The framework begins with an LLM-driven social media data augmentation strategy, employing prompt orchestration to generate diverse yet semantically consistent misinformation samples. These augmented samples are integrated into a CL-based detector, where the semantic richness and diversity introduced by the LLM enhance the CL's discriminative feature extraction and predictive capability, thus improving generalization beyond the original training distribution. To align with CL's discriminative goal, we develop a contrastive loss-aware joint training and fine-tuning mechanism, in which CL's representation learning constrains LLM hallucinations and guides augmentation quality. Through this closed-loop optimization, the CL-based detector progressively absorbs latent semantic knowledge from the LLM, effectively overcoming semantic complexity and reducing erroneous generations. Experimental results on four benchmark datasets (Twitter15, Twitter16, Weibo, and PHEME) demonstrate that LACL consistently outperforms mainstream deep learning methods and surpasses approaches that directly apply commercial LLMs for detection without task-specific adaptation. These gains are observed across different backbone LLMs (Qwen and Llama), underscoring LACL's robustness, adaptability to diverse language contexts, and superior generalization capability.**

***Index Terms*—Misinformation detection, large language models, contrastive learning, fine-tuning, social networks.**

I. Introduction

The rapid expansion of the Internet has made information dissemination more convenient and facilitated the spread of misinformation, leading to significant societal challenges, including public confusion and even panic [1]. In response, social media platforms have implemented measures like manual content review and account restrictions, which, while effective to some extent, are costly and susceptible to bias. To enhance detection efficiency, deep neural networks (DNNs) have been increasingly employed, leveraging both supervised [2], [3] and semi-supervised methods [4], [5].

Although supervised learning has achieved promising results, its heavy reliance on large-scale labeled datasets and its inability to adapt to rapidly evolving rumor patterns limit its long-term effectiveness. Label annotation in this domain is costly and time-consuming. To address these limitations, contrastive learning (CL), a promising self-supervised learning approach, has shown great potential in tasks like semantic segmentation [6], text classification [7], and named entity recognition [8]. When combined with graph neural networks (GNNs) [9], [10], CL enhances misinformation detection by extracting features from complex data structures, improving the analysis of content propagation in social networks.

The emotions and opinions expressed by social media users are essential for assessing content authenticity [11]. User-generated content, like microblog interactions, reveals how misinformation spreads and helps understand its dynamics within networks. However, existing CL-based methods, such as DropEdge [12], AdaEdge [13], and NodeAug [14], which integrate GNNs, focus on misinformation propagation and network structure, often overlooking emotional context and diverse opinions. Similarly, natural language processing (NLP) techniques like synonym replacement [15] improve text-level representation but struggle to capture subtle emotions, sarcasm, and cultural cues, limiting their effectiveness in capturing emotional responses, underlying motivations, and subtle cues such as sarcasm or cultural context.

Large language models (LLMs) have transformed NLP by leveraging vast parameter scales and extensive pre-training to achieve superior language understanding and capture subtle semantic nuances [16], [17]. These capabilities enable LLMs to identify misinformation patterns, implicit logic, and inconsistencies, making them powerful tools for rumor detection. However, directly applying LLMs is prone to generating hallucinations [18], [19], producing plausible content but factually incorrect. This inherent risk of LLM hallucination is a critical challenge, especially when employing LLMs for data augmentation in sensitive domains like misinformation detection, as it can lead to the generation of misleading or counterproductive training samples. LLMs are also limited by training data biases and struggle to adapt to rapidly evolving rumor content. To address these limitations, including the propensity for hallucination, LLMs' advanced feature extraction and semantic understanding capabilities are synergistically combined with CL. While CL serves as the core detector by learning robust representations, LLMs enhance performance through diverse, semantically aligned augmentation. Importantly, a CL-guided fine-tuning strategy mitigates hallucinations and aligns LLM outputs with CL objectives.

Manuscript received XX January 2024; revised XX XXX 2025; accepted XX XXX 2025. This work was supported in part by the National Natural Science Foundation of China under Grants 61502230, 61501224, and 62202221, in part by the Natural Science Foundation of Jiangsu Province under Grants BK20201357 and BK20220331, and in part by the Six Talent Peaks Project in Jiangsu Province under Grant RJFW-020. The Associate Editor for this article was XXX. (Corresponding author: Yuanfei Dai.)

Hang Shen, Xu Wang, Yuanfei Dai, Tianjing Wang, and Guangwei Bai are with the College of Computer and Information Engineering (College of Artificial Intelligence), Nanjing Tech University, Nanjing, 211816, China. E-Mail: {hshen, daiyuanfei, wangtianjing, bai}@njtech.edu.cn, Lhasahi@163.com

Digital Object Identifier XXX

A. Challenges and Related Works

Despite the considerable potential, the collaboration between LLMs and CL faces several pressing challenges.

1) Leveraging LLMs to Overcome Data: Limitations in the CL framework, including the use of existing detection datasets often drawn from a single social platform, limit model generalization across multiple sources. Traditional CL-based data augmentation techniques, such as synonym replacement and sentence rearrangement [15], can expand the dataset size but often fail to capture nuanced semantic features like sarcasm, metaphors, and implicit suggestions, sometimes even producing misleading samples. Moreover, rumor propagation is strongly shaped by social contexts and event backgrounds, but conventional methods fail to model, limiting their ability to capture subtle variations in collective behavior. Feng et al. [20] employed bidirectional multi-level graph CL with data augmentation to enhance rumor detection. However, the method struggles to capture fine-grained semantics in complex contexts and performs less effectively across diverse cultural backgrounds due to its inability to preserve distinct rumor styles and propagation patterns. In [21], LLM-enhanced news reframing was used to inject stylistic diversity. Each news article was transformed into multiple stylistic variations during training to increase data diversity and help the student network learn robust features, which can be seen as a form of unidirectional knowledge transfer from the LLM. However, efficient data utilization and effective collaboration between the teacher LLM and the student remain to be explored.

2) Deep Extraction of Representations with Limited Samples: Effectively extracting deep semantic representations in social media rumor detection remains challenging due to the scarcity of samples in current public datasets. Traditional data augmentation methods [12]–[15] partially mitigate this issue but primarily focus on shallow text transformations, failing to achieve substantial semantic enhancement. Thus, CL frameworks may struggle to capture deep semantic features in rumor texts, such as discourse logic, argument structure, and emotional inclination, when constructing positive and negative sample pairs. Moreover, rumor texts often involve complex contextual dependencies and implicit semantic links, which require deep semantic understanding and representation learning. Liu et al. [22] proposed a fake news detection framework that enhances news graph representation by integrating content, emotional information, and dissemination structure using GNNs and edge-aware techniques. However, under low-sample conditions, the framework struggles to extract deep semantic and emotional features effectively, limiting its generalization and early detection accuracy. Thus, a key challenge is to extract deep semantic features from limited samples using advanced augmentation and optimized CL training.

3) Synergy of LLMs and CL: DNN models, including CL, can be integrated through joint training or model concatenation [23]. One straightforward approach is to leverage LLMs' language understanding capabilities for detection tasks. However, due to misalignment, these methods struggle to harness LLMs' language understanding strength and CL's feature extraction potential. Hu et al. [24] proposed a fake news detection method that utilizes ChatGPT as an advisor rather than a detector, providing multi-perspective reasoning and guidance. CALRec [25], a sequential recommendation framework, uses two-stage LLM fine-tuning to align user interaction sequences and target items, enhancing model performance by maximizing positive sample similarity and minimizing negative sample similarity. Dong et al. [26] proposed an unsupervised LLM alignment method for information retrieval, utilizing proximal policy optimization (PPO) to optimize LLM parameters. Jiang et al. [27] introduced CL to enhance multimodal LLMs by treating hallucinated text as hard negatives. This brings non-hallucinated text and visual samples closer while separating non-hallucinated and hallucinated text. In [28], LLMs were used to extract keywords and assess their relationship weights through graph Laplacian learning to automatically construct a knowledge graph (KG). MiLk-FD [29] effectively integrates the semantic and structural features of news content with factual knowledge from multiple KGs, resulting in superior performance in fake news detection. While these approaches utilize LLMs as data augmentation and KG extraction tools, they lack direct interlinking and feedback mechanisms. Thus, a challenge remains in designing a sustainable optimization method that enables the synergy of LLMs and CL.

B. Contributions and Organization

To address the aforementioned challenges, we propose LACL (LLM-Augmented Contrastive Learning), a framework designed to enhance the stability and accuracy of fake news detection in social networks. In this framework, the LLM's advanced language understanding and generation capabilities compensate for the feature extraction limitations of a CL-based detector, while CL's discriminative learning improves LLM fine-tuning and data augmentation. The key contributions of this study are threefold:

- An LLM-based data augmentation method is developed to overcome social network data limitations. This method leverages the LLM's knowledge to generate diverse and semantically consistent misinformation samples, expanding the training dimension of the CL-based detector.
- A LLM-assisted feature extraction and label prediction method is designed, leveraging the LLM's semantic understanding and sample generation capabilities to enhance CL's ability to capture deeper representations.
- To align the LLM with the CL's discriminative objective, we develop a sustainable joint training and fine-tuning strategy. The contrastive loss guides LLM fine-tuning and augmentation strategy updates, where the generated high-quality data is leveraged to strengthen CL's feature extraction and classification capabilities. This closed-loop optimization enables the CL-based detector to progressively extract implicit knowledge from the LLM, overcoming its limitations in handling complex semantics.

Experimental results on multiple mainstream social media datasets highlight LACL's effectiveness, robustness, and applicability. The research questions addressed include:

- Can LACL consistently outperform the performance upper bound of CL baseline methods?

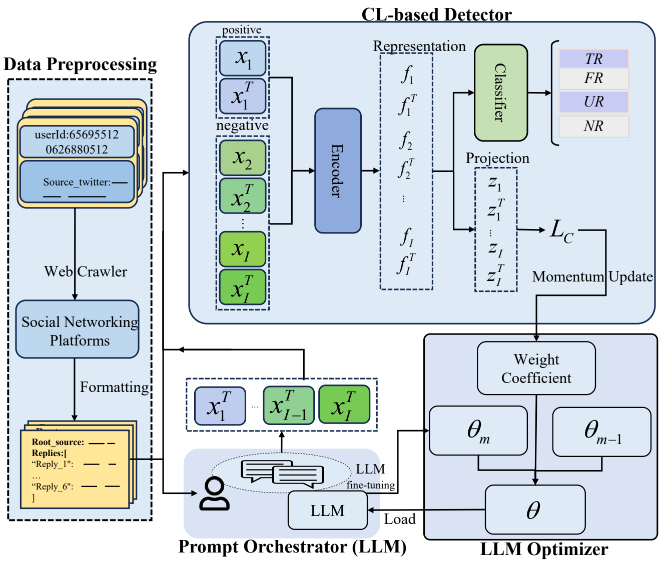

Fig. 1. LACL architecture.

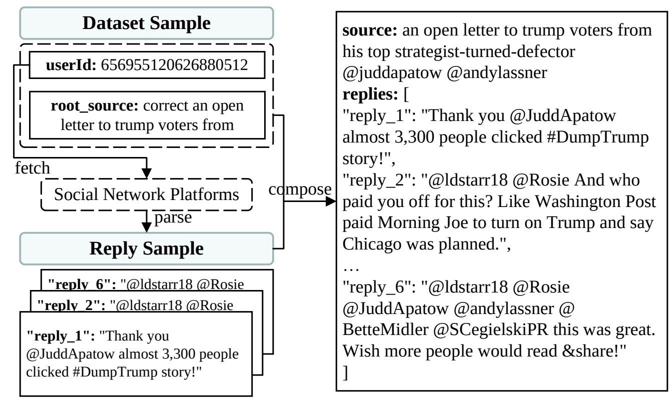

Fig. 2. Data preprocessing examples.

- What impact do data augmentation rounds and base LLM parameter size have on detection performance?
- Can multi-round LLM fine-tuning continue to improve performance, and do marginal effects exist?

The remainder of this paper is organized as follows. Section II introduces the LACL architecture, which includes data preprocessing and prompt engineering, feature extraction and label prediction, and CL-LLM alignment. Section III presents datasets, base LLM, and benchmark method selection, as well as experimental setup. Section IV analyzes the experimental results and highlights key findings. Finally, Section V concludes the paper and discusses potential future directions.

II. Proposed Method

Fig. 1 illustrates the LACL architecture, a framework designed to detect false content in social networks by fostering a symbiotic relationship between a CL-based detector and an LLM optimizer. This architecture, comprising a data preprocessing module, a prompt orchestrator, a CL-based detector, and an LLM optimizer, is founded on the principle that CL and the LLM can mutually enhance each other. The LLM's role in generating high-quality augmented data is crucial for overcoming data scarcity, while the detector's discriminative capabilities are leveraged not only for misinformation detection but also to provide a strong feedback signal for refining the LLM's generation strategy, thereby minimizing issues like LLM hallucinations. This iterative refinement process aims to improve the quality of LLM-generated samples, which, in turn, enhances the detector's unsupervised classification performance. Conversely, the improved classification performance, as reflected through the contrastive loss function, provides a clearer guiding signal for the LLM's augmentation strategy. The workflow for this collaboration is divided into the following three stages:

1) *Data Preprocessing and Prompt Orchestration*: Raw data is scraped from social networks using web crawlers and formatted accordingly. The processed data is fed into the prompt orchestrator, which generates high-quality augmented data to expand the CL's training dimension.
2) *LLM-Assisted Feature Extraction and Label Prediction*: Augmented data is paired with the original data and input into the CL network to extract features and predict labels. After training, the CL model's parameters are frozen, and during testing, the classifier processes the extracted features to predict labels.
3) *Contrastive Loss-Aware Joint Fine-Tuning and Training*: The contrastive loss is leveraged to guide LLM fine-tuning, ensuring its outputs align with CL's discriminative capability. This alignment specifically improves the LLM's generation strategy and indirectly optimizes the feature extraction of the CL-based detector.

A. Data Preprocessing and Prompt Orchestration

Fig. 2 illustrates the structure of each data instance, which typically includes the original post and its associated responses. The predefined prompt guides and constrains the LLM to ensure it can recognize and analyze typical characteristics of misinformation in social networks, such as logical incoherence, factual inaccuracies, strong emotional tone, and noticeable biases. Through this guidance, the LLM can capture subtle clues in the original data that may indicate content manipulation, thereby accurately identifying potential misinformation. While this prompt orchestration provides initial directional guidance to the LLM, the primary mechanism for robustly controlling semantic integrity and minimizing potential hallucinations during the augmentation process is the subsequent CL-guided LLM fine-tuning, as detailed in Section II-C. Once the analysis is complete, the LLM reorganizes and diversifies the original content to generate semantically consistent, varied augmented data.

The prompt orchestration should satisfy the following objectives:

- *Holistic Augmentation*: Augment data from a global perspective to effectively capture the dataset's overall features and distribution.
- *Format Consistency*: Ensure generated outputs adhere to the original data format, maintaining structural integrity for seamless integration.

This article has been accepted for publication in IEEE Transactions on Computational Social Systems. This is the author's version which has not been fully edited and content may change prior to final publication. Citation information: DOI 10.1109/TCSS.2025.3599080

You are given data from a rumor detection dataset, and your task is to enhance the data based on the following instructions:
1. **Holistic Enhancement**:
- Enhance the data by considering its overall content, not just focusing on isolated parts. Make sure the enhancements reflect a comprehensive understanding of the entire data piece.
2. **Maintain Format Consistency**:
- Ensure the enhanced data retains the exact same format as the original data. No structural changes should occur.
3. **Increase Diversity**:
- Focus on making the data more diverse in terms of language expression, without altering the underlying meaning. The enhanced data should be more varied but semantically identical to the original.
4. **Preserve Semantics**:
- It is critical that the enhanced data preserves the exact same meaning as the original, even though the expressions may differ.

Fig. 3. Prompt orchestration example.

- *Content Diversity*: Encourage varied content generation, enhancing richness while preserving authenticity.
- *Semantic Alignment*: Maintain semantic consistency between the augmented and original data, preserving meaning critical for accurate misinformation detection.

Following these principles, we designed the prompt illustrated in Fig.3, ensuring that each requirement is met in practice. As shown in Fig. 4, the augmented content not only restructures sentences as a whole to better capture global semantics. For example, rewriting "an open letter to Trump voters from his top strategist-turned-defector" as "A public letter to Trump supporters from his former strategist-turned-critic", but also preserves the original data format, including identical fields and hierarchical reply structures, ensuring compatibility with downstream processing. The language style is diversified while retaining the original meaning, such as changing "They love him" to "They're fully committed to him" for greater specificity. Moreover, the semantic core remains intact; for instance, "She obviously didn't look at all the havoc Drumpf has caused. He destroyed the USFL!" becomes "She clearly ignored all the damage Trump has already done. He ruined the USFL!", maintaining the critical tone and factual references while refining the phrasing for clarity. These examples collectively demonstrate that the prompt design effectively enhances data quality and diversity while ensuring structural and semantic consistency with the original dataset.

B. LLM-Assisted Feature Extraction and Label Prediction

A social network dataset containing I instances is represented as $\{x_1, x_2, \ldots, x_I\}$, where x_i denotes the i-th instance, with each instance processed by the LLM. The transpose of the feature vector for the i-th instance is represented as x_i^T, which is used in various operations such as similarity computation and feature projection. Using a predefined prompt, the LLM generates augmented data that maintains semantic consistency but differs in expression. The CL detector comprises a feature extraction network based on BERT (Bidirectional Encoder Representations from Transformers) [30] and a projection head built on a multilayer perceptron [31] for feature extraction. The feature representation of x_i is denoted as f_i. Let W_1 represent the weight matrix of the first layer of the MLP, which maps input features f_i to the hidden layer, and W_2 represent the weight matrix of the second layer, which maps the hidden layer output to the final representation z_i. This process is expressed


```
{
    "uid": "bdf404b551618b1fbff4b9f17c0829ba",
    "string_value": "an open letter to trump voters from his top strategist-turned-defector URL via",
    "replies": [
      {
        "reply_1": "It won't matter. They love him.",
        "reply_2": "Excuses. Why so angry? What's wrong w America now, beyond idiots drawn to a hateful demagogue?",
        "reply_3": "Kudos! You are now enlightened--albeit much later than we with much less political acumen.",
        "reply_4": "Sometimes it is hard to see the light in the forest. Happy to be in the light!",
        "reply_5": "have you a solution? Or was this just a cathartic bit of self-flagellation?",
        "reply_6": "Yes but way too late! She obviously didn't look at all the havoc Drumpf has caused. He destroyed the USFL!",
        "reply_7": "Reagan is the nexus of problems with USA today. Trickle down failed. Grover Norquist is evil!",
        "reply_8": "Thank you for sharing my piece back in March. It means so much from someone I admire!"
      }
    ],
}
```


output


```
{
  "uid": "bdf404b551618b1fbff4b9f17c0829ba",
  "string_value": "A public letter to Trump supporters from his former strategist-turned-critic URL via",
  "replies": [
    {
      "reply_1": "It won't make a difference. They're fully committed to him.",
      "reply_2": "Just excuses. Why the outrage? What's truly wrong with America now, besides those following a divisive demagogue?",
      "reply_3": "Bravo! You've finally seen the light—although a bit later than some of us with less political insight.",
      "reply_4": "It's not always easy to find clarity in the chaos. Glad to be here in the light!",
      "reply_5": "Do you have a solution, or was this just a therapeutic rant?",
      "reply_6": "Yes, but it's far too late! She clearly ignored all the damage Trump has already done. He ruined the USFL!",
      "reply_7": "Reagan is at the root of today's issues in America. Trickle-down economics failed. Grover Norquist is a menace!",
      "reply_8": "Thanks for sharing my article back in March. It means a lot, especially from someone I respect!"
    }
  ]
}
```


Fig. 4. Data augmentation example.

as a nonlinear transformation, $z_i = g(f_i)$. Let $\sigma(\cdot)$ denote the activation function. The transformation can be written as

$$z_i = W_2 \sigma(W_1 f_i). \tag{1}$$

In the projection space, the similarity function to measure the similarity between z_i and $z_{i'}$ is defined as

$$\mathrm{sim}(z_i, z_{i'}) \triangleq \frac{z_i \cdot z_{i'}}{\|z_i\| \, \|z_{i'}\|}. \tag{2}$$

The samples involved in the loss calculation include both the original samples and their augmented counterparts, resulting in a total of $2I$ samples. The projection representation of x_i^T is denoted as z_i^T. Applying (2) to the InfoNCE Loss [32], the contrastive loss at the n-th epoch is described as

$$\mathcal{L}_n = -\frac{1}{2I} \sum_{i=1}^{I} \log \frac{\exp\left(\mathrm{sim}\left(z_i, z_i^T\right)/\tau\right)}{\sum\limits_{i'=1, i' \neq i}^{2I} \exp\left(\mathrm{sim}\left(z_i, z_{i'}\right)/\tau\right)}, \tag{3}$$

where τ is the temperature hyperparameter. Minimizing (3) encourages samples from the same class to cluster closely in the projection space while increasing the distance between samples of different classes. By utilizing the contrastive loss as a potent feedback signal, the LLM is guided to generate augmented samples that are not only diverse but also discriminatively valuable for the CL detector. This process inherently penalizes and reduces the generation of factually inconsistent, semantically drifting, or otherwise misleading augmented data that could be characterized as hallucinations.

The classifier in the CL-based detector is defined as $f : G \rightarrow Y = \cup_{c \in \{1,2,\ldots,C\}} y_c$, where C represents the number of label categories and the labels $y_c \in \{NR, FR, TR, UR\}$ with *NR* representing Non-Rumor, *FR* False Rumor, *TR* True Rumor, and *UR* Unverified Rumor. This classifier comprises a fully connected layer followed by a softmax activation function. During the testing phase, the extracted feature representations are fed into the classifier for category prediction.

In each batch, we treat x_1 and its augmented counterpart

This article has been accepted for publication in IEEE Transactions on Computational Social Systems. This is the author's version which has not been fully edited and content may change prior to final publication. Citation information: DOI 10.1109/TCSS.2025.3599080

x_1^T as positive samples, since they are semantically similar, both stemming from the same original instance but with varied expressions. $\{x_2, \ldots, x_I\}$ and their augmented versions $\{x_2^T, \ldots, x_I^T\}$ are considered negative samples as they originate from different instances and hence are semantically dissimilar. The CL network's feature extractor processes these positive and negative pairs to generate their initial feature representations. As described in (1), the features are mapped into a shared feature space to optimize data distribution, ensuring that semantically similar points are brought closer, while dissimilar ones are pushed apart. Cosine similarity is used to quantify the similarity between feature vectors.

Once the feature extraction training is completed, the feature extractor is frozen. During the testing phase, new data is input into this frozen feature extractor. The extracted features are passed into the pre-trained classifier, which maps them to the predefined categories of rumors. The final prediction outputs the labels, completing the rumor classification process.

Algorithm 1: Merge (θ_m,θ_{m-1},θ_0, λ_{m-1}, λ_m, α)

Input: θ_m, θ_{m-1}, θ_0, λ_{m-1}, λ_m, α
Output: θ
1 **foreach** $r \in \{m-1, m\}$ **do**
2 $\quad \vartheta_r \leftarrow \theta_r - \theta_0$;
3 $\quad \hat{\vartheta}_r \leftarrow Top(\vartheta_r, q)$;
4 $\quad \hat{\vartheta}_r \leftarrow \hat{\gamma}_r \odot \hat{\eta}_r$;
5 $\quad \gamma_r \leftarrow \operatorname{sgn}(\hat{\vartheta}_r)$;
6 $\quad \eta_r \leftarrow |\hat{\vartheta}_r|$;
7 $\quad$ **for** $e \in dim(\theta_0)$ **do**
8 $\qquad \gamma^{(e)} \leftarrow \operatorname{sgn}(\hat{\vartheta}_{m-1}^{(e)} + \hat{\vartheta}_m^{(e)})$;
9 $\qquad \mathcal{R}^{(e)} \leftarrow \{r \in \{m-1, m\} | \hat{\gamma}_r^{(e)} = \gamma^{(e)}\}$;
10 $\qquad \vartheta^{(e)} \leftarrow \frac{1}{|\mathcal{R}^{(e)}|} \sum_{r \in \mathcal{R}^{(e)}} \lambda_r \hat{\vartheta}_r^{(e)}$;
11 $\theta \leftarrow \theta_0 + \alpha\vartheta$;
12 **return** θ;

C. Contrastive Loss-Aware Joint Fine-Tuning and Training

In this study, the LLM was strategically and progressively employed to enhance and diversify social network datasets rather than being directly involved in feature extraction or classification. This subsection presents a joint fine-tuning and training mechanism. The augmented data generated by the LLM continually expands and enriches the training dataset, strengthening the CL detector's feature extraction and classification in subsequent training rounds.

Mainstream LLM fine-tuning methods include full fine-tuning [33], prompt learning [34], and parameter-efficient fine-tuning (PEFT) [35]. Among PEFT methods, low-rank adaptation (LoRA) [36] achieves efficient parameter updates by adding low-rank decomposition matrices alongside the original weight matrices. Based on LoRA, we introduce a bootstrapped LLM fine-tuning method for data augmentation.

Let θ_0 denote the initial LLM. Before the m-th fine-tuning, θ_{m-1} is used for data augmentation, implying that the dataset and model parameters evolve iteratively through the fine-tuning process. The entire training process consists of N epochs, and the LLM is fine-tuned periodically at the end of the n-th epoch. Denote the dataset at the end of the n-th epoch after the m-th fine-tuning as $\mathcal{D}_{n,m}$. Based on $\mathcal{D}_{n,m}$ and θ_0, the LLM fine-tuned in the m-th iteration is represented as

$$\theta_m = LoRA\left(\mathcal{D}_{n,m}, \theta_0\right). \tag{4}$$

The update vector is computed as $\vartheta_{m-1} = \theta_{m-1} - \theta_0$ (similarly, $\vartheta_m = \theta_m - \theta_0$). Each entry in ϑ_{m-1}, which exists in a $dim\left(\theta_0\right)$ dimensional space, can be considered an axis, where the sign of the parameter indicates the direction along the axis. Consequently, ϑ_{m-1} can be decomposed into a sign vector $\gamma_{m-1} \in \mathbb{R}^{dim(\theta_0)}$ and a magnitude vector $\eta_{m-1} \in \mathbb{R}^{dim(\theta_0)}$, expressed as $\vartheta_{m-1} = \gamma_{m-1} \odot \eta_{m-1}$, where $\odot$ denotes element-wise multiplication. Formally, $\gamma_{m-1} = \operatorname{sgn}(\vartheta_{m-1})$ and $\eta_{m-1} \triangleq |\vartheta_{m-1}|$. $\operatorname{sgn}(\vartheta_{m-1})$ returns $+1$, 0, or -1 depending on the sign of ϑ_{m-1}, and $\operatorname{sgn}(\vartheta_{m-1}) \cdot |\vartheta_{m-1}| = \vartheta_{m-1}$.

The joint fine-tuning process, detailed in Algorithm 1, consists of the following three key steps:

1) *Trimming.* ϑ_{m-1}, to be merged, is first trimmed to remove redundant values, yielding $\hat{\vartheta}_{m-1}$. To eliminate redundancy, the top $q\%$ of the magnitudes in ϑ_{m-1} are retained, while the rest are set to 0 (see line 3). Subsequently, $\hat{\vartheta}_{m-1}$ is decomposed into the sign vector $\hat{\gamma}_{m-1}$ and the magnitude vector $\hat{\eta}_{m-1}$ (see line 4). A similar procedure is applied to θ_m.
2) *Sign Election.* For each e-th entry in $\hat{\gamma}_{m-1}$, $\hat{\vartheta}_{m-1}$, and $\hat{\eta}_{m-1}$, the values are denoted as $\hat{\gamma}_{m-1}^{(e)}$, $\hat{\vartheta}_{m-1}^{(e)}$, and $\hat{\eta}_{m-1}^{(e)}$. Let ϑ denote the aggregated task vector, with its sign vector as γ. Resolving sign conflicts between θ_{m-1} and θ_m is a prerequisite for their merging (line 8). To achieve this, the e-th entry of γ is computed as
$$\gamma^{(e)} = \operatorname{sgn}(\hat{\vartheta}_{m-1}^{(e)} + \hat{\vartheta}_m^{(e)}). \tag{5}$$
3) *Weighted Disjoint Merge.* For the e-th parameter in ϑ, denoted as $\hat{\vartheta}_r^{(e)}$, only the value from the model with a sign consistent with $\gamma^{(e)}$ is retained. Denoted by $\mathcal{R}^{(e)} = \{r \in \{m-1, m\} | \hat{\gamma}_r^{(e)} = \gamma^{(e)}\}$ the index set. The e-th parameter of ϑ is computed as
$$\vartheta^{(e)} = \frac{1}{|\mathcal{R}^{(e)}|} \sum_{r \in \mathcal{R}^{(e)}} \lambda_r \hat{\vartheta}_r^{(e)}, \tag{6}$$
where $\theta_r^{(e)}$ belongs to $\{\theta_{m-1}^{(e)}, \theta_m^{(e)}\}$ and λ_r is θ_r's weight, determined by the Contrastive loss. The merged LLM is expressed as
$$\theta = \theta_0 + \alpha\vartheta, \vartheta = [\hat{\vartheta}^{(1)}, \hat{\vartheta}^{(2)}, ..., \hat{\vartheta}^{(dim(\theta_0))}]^T, \tag{7}$$
with α being a hyperparameter.

The LLM–CL alignment is embedded into a joint training framework, as outlined in Algorithm 2. LLM-driven augmentation is performed every T epochs, yielding $W = \lceil \frac{N}{T} \rceil$ augmentation cycles over N epochs. During training, contrastive loss guides the LLM fine-tuning process, effectively suppressing hallucinations from obvious factual errors to subtle misleading cues, by penalizing generations that impair the CL's discriminative ability. This iterative feedback loop enables

Algorithm 2: Alignment (θ_0, θ_m, θ_{m-1}, λ_{m-1}, λ_m, α, $\mathcal{L}_n$, $\mathcal{D}_{n,m}$, m, n)

Input: θ_0, θ_m, θ_{m-1}, λ_{m-1}, λ_m, α, $\mathcal{L}_n$, $\mathcal{D}_{n,m}$, m, n
Output: θ
1 **if** $n \leq N$ **then**
2   **foreach** $n \in \{1, 2, \ldots, N\}$ **do**
3         $\varphi_n \leftarrow \mu \mathcal{L}_n + (1-\mu) \frac{1}{n-1} \sum_{n'=1}^{n-1} \mathcal{L}_{n'}$;
4         $\lambda_m \leftarrow \frac{\varphi_m}{\sum_{m'=1}^{m} \varphi_{m'}}$;
5     $\theta_m \leftarrow LoRA\,(\mathcal{D}_{n,m}, \theta_0)$;
6     $\theta \leftarrow$ Merge $(\theta_{m-1}, \theta_m, \theta_0, \lambda_{m-1}, \lambda_m, \alpha)$;
7     $\theta_{m-1} \leftarrow \theta$;
8     $\mathcal{D}_{n,m} \leftarrow$ Train (θ);
9   **if** $m \leq M$ **then**
10   Alignment (θ_0, θ_m, θ_{m-1}, λ_{m-1}, λ_m, α, $\mathcal{L}_n$, $\mathcal{D}_{n,m}$, m, n);
11         $\lambda_{m-1} \leftarrow \lambda_m$;
12         $m \leftarrow m + 1$;
13   **else**
14   **return**;

the LLM to progressively refine its augmentation strategy, producing samples that are both semantically consistent and performance-enhancing.

This contrastive loss is also central to our hallucination mitigation strategy. If the LLM produces augmented data that is a product of hallucination (e.g., containing factual inaccuracies, deviating semantically from the original sample's class, or introducing misleading characteristics that obscure true class features), such samples will likely be poorly discriminated by the CL network. This poor discrimination translates to a higher Ln. This error signal is then directly used to adjust the LLM's parameters during the fine-tuning phase (Algorithms 1 and 2), effectively steering the LLM away from generating such problematic augmentations in subsequent rounds. The loss value, $\mathcal{L}_n$, as in (3), quantifies the CL model's ability to learn distinguishing misinformation features and reflects the quality of the LLM-augmented data. A smaller $\mathcal{L}_n$ indicates that the augmented data is semantically rich and discriminative, allowing the CL model to effectively distinguish between positive and negative samples; otherwise, performance degrades. By monitoring $\mathcal{L}_n$, the algorithm dynamically adjusts the adapter parameter fusion during the predefined fine-tuning rounds. To prevent the undue impact from $\mathcal{L}_n$ in a single epoch, a momentum update strategy [37] is employed to evaluate the LLM's augmentation effect (see lines 3–4), expressed as

$$\varphi_n = \mu \mathcal{L}_n + (1-\mu) \frac{1}{n-1} \sum_{n'=1}^{n-1} \mathcal{L}_{n'}, \tag{8}$$

where μ is the influence factor. Based on φ_n, the weight for the m-th fine-tuning is adjusted as

$$\lambda_m = \frac{\varphi_m}{\sum_{m'=1}^{m} \varphi_{m'}}. \tag{9}$$

By calling LoRA (line 5), a customized LLM, θ_m, is generated, and then, by calling Algorithm 1, the fine-tuned LLM is integrated to produce an optimized LLM (line 6). M determines the maximum LLM fine-tuning rounds (lines 10–15). When $m > M$, the algorithm halts fine-tuning. M can be manually adjusted as needed.

This alignment process forms a robust, mutually reinforcing feedback loop between the LLM and the CL detector. Leveraging the LLM's semantic understanding and generative capabilities, diverse augmented data is produced to enrich the CL detector's training and improve its capacity for capturing complex semantics. In return, contrastive loss offers a direct, quantitative signal of data quality, guiding the LLM's fine-tuning to reduce hallucinations and generate samples that strengthen the unsupervised classification. This symbiotic cycle ensures that both components evolve to overcome their respective limitations, driving continuous optimization of the entire detection framework.

III. Experimental Preparation

A. Dataset Selection

In the experiments, four benchmark datasets widely used in social media misinformation detection were selected: Twitter15 [38], Twitter16 [38], Weibo [39], and PHEME [40]. Specifically, Twitter15 and Twitter16 contain 1,490 and 818 source tweets, respectively, and support four-class rumor detection, including *TR*, *FR*, *NR*, and *UR* categories. The Weibo and PHEME datasets support binary classification, consisting of 9,128 and 5,922 instances, respectively. The Weibo dataset includes 4,640 samples labeled as False and 4,488 as True, while PHEME includes 3,006 False and 2,916 True instances. To enhance contextual richness for inference, original posts along with all associated replies were collected via web crawling from the corresponding social media platforms. For data partitioning, a standard split was adopted: 70% for training, 20% for testing, and 10% for validation, ensuring a comprehensive and reliable evaluation setting.

B. Comparative Methods

To comprehensively evaluate the proposed framework, eight representative algorithms were selected as baselines:

- **BiGCN** [41]: Employs GNNs to capture rumor diffusion in both top-down and bottom-up directions.
- **BiMGCL** [20]: Leverages a bidirectional graph structure and multi-level CL to model rumor propagation, reducing dependence on labeled data and improving detection through diverse graph structures.
- **LSTM** [42]: Captures long-range dependencies via gating mechanisms, effective for sequential and semantic rumor modeling.
- **Text-CNN** [43]: Employs CNN with multi-scale convolutional filters to extract discriminative local semantic patterns efficiently for text classification.
- **RCNN** [44]: Combines CNN-based local feature extraction and RNN-based global context modeling to effectively detect rumors.

TABLE I
CATEGORIZATION OF PROPOSED METHODS

Classification of Proposed Methods	Choices of base LLM and model size				Data Augmentation Rounds & Fine-tuning Times (W, M)				
	Qwen-7B	Qwen-14B	Llama-7B	Llama-13B	$(1,0)$	$(2,0)$	$(3,0)$	$(3,1)$	$(3,2)$
Proposed-1	✓				✓				
Proposed-2	✓					✓			
Proposed-3	✓						✓		
Proposed-4	✓							✓	
Proposed-5	✓								✓
Proposed-6		✓					✓		
Proposed-7			✓		✓				
Proposed-8			✓					✓	
Proposed-9				✓			✓		

- **HAN** [45]: Utilizes dual-level attention mechanisms (word and sentence) to capture hierarchical text features, enhancing rumor detection interpretability.
- **ELKP** [46]: Enhances language models via knowledge-driven prompting and external knowledge injection, improving semantic reasoning and adaptability for misinformation detection.
- **SRD-PSID** [47]: Leverages contrastive self-supervised learning of heterogeneous social and semantic patterns, enriching rumor representation and detection accuracy.

To assess the impact of different strategies on performance, we examine the framework across three key dimensions: the choice of base LLM (Qwen [48] vs. Llama [49]), the number of data augmentation rounds (1–3), and the number of fine-tuning rounds (none, 1, or 2). These dimensions are critical for understanding how varying LLM sizes and augmentation strategies influence detection. Table I summarizes nine proposed configurations based on these factors:

- **Proposed-1, -2, and -3**: Utilize Qwen-7B as the base LLM, with 1, 2, and 3 data augmentation rounds, respectively, and no fine-tuning.
- **Proposed-4 and -5**: Also use Qwen-7B, but add 1 or 2 fine-tuning rounds in addition to data augmentation.
- **Proposed-6 and -9**: Uses a larger Qwen-14B base LLM with 3 data augmentation rounds to assess the impact of a larger model on performance.
- **Proposed-7 and -8**: Employ Llama models with size of 7B, exploring different combinations of data augmentation rounds and fine-tuning times.

C. Experimental Design and Configuration

We examined the impact of data augmentation, LLM fine-tuning, and different types and parameter amounts of base LLMs. The first experiment utilized CL baselines to evaluate LACL's performance boundary. The second focused on analyzing how augmentation rounds influence detection performance. The third assessed the impact of fine-tuning rounds (representing training costs). The fourth examines resource usage.

Two widely recognized evaluation metrics were employed to quantitatively analyze and assess the performance of rumor detection methods in social networks, i.e.,

$$\text{Accuracy} = \frac{TP + TN}{TP + TN + FP + FN} \tag{10}$$

and

$$F1 = \frac{2 \times TP}{2 \times TP + FP + FN}. \tag{11}$$

TP, *TN*, *FP*, and *FN* represent true positives, true negatives, false positives, and false negatives, respectively. Accuracy provides an intuitive measure of correctly identified instances' proportions, while the F1 score emphasizes the balance between precision and recall, highlighting the proportion of correctly classified instances.

TABLE II
DEFAULT PARAMETER SETTINGS

Parameter	Value
Batch size	256
Training epochs (N)	25
Augmented cycles (T)	10
Magnitude filtering ratio (q)	top 20%
LLM-fusion hyperparameter (α)	1
Influence factor (μ)	0.99
Maximum LLM fine-tuning rounds (M)	2
LoRA rank	8
LoRA learning rate	5×10^{-5}
LoRA training epochs	5

Key hyperparameters, learning rate, training epochs, and batch size were kept consistent throughout the experiments to ensure a fair evaluation. Detailed training parameters were set as shown in Table II. This value of q controls the magnitude filtering process, where the top 20% of the most significant features are selected during training. A value of $\alpha = 1$ indicates a balanced model fusion. In light of the dataset size and label distribution, LoRA hyperparameters were selected to promote robust convergence and generalization. A learning rate of 5×10^{-5} was selected for LoRA (rank = 8) to balance gradient stability and task adaptation.

Tests ran on a high-performance server featuring an Intel Core i9-14900K processor, 64GB DDR5 5200MHz RAM, a 4TB PCIe 4.0 SSD, an ASUS PRIME Z790-P WIFI D5 motherboard, and dual Gigabyte RTX 4090 24GB GPUs.

TABLE III
GPT-4O DIRECT DETECTION ACCURACY (%) ON TWITTER15 AND 16

Dataset	TR	NR	FR	UR	Avg Acc
Twitter15	37.15	31.89	42.36	39.04	37.61
Twitter16	32.18	38.94	41.57	43.09	38.94

TABLE IV
GPT-4O DIRECT DETECTION ACCURACY (%) ON WEIBO AND PHEME

Dataset	True	False	Avg Acc
Weibo	58.37	45.92	52.15
PHEME	63.45	49.18	56.32

IV. RESULT ANALYSIS

A. Performance Bound Analysis

Note that LACL does not rely on directly using LLMs for misinformation detection. Instead, it leverages the semantic understanding and generation capabilities of LLMs to augment the CL-based detector in a task-aware, domain-adaptive manner. To contextualize the performance bounds of our method, we first conducted a preliminary study by directly applying GPT-4o[1], a mainstream LLM, to detect misinformation in social media content. Specifically, we randomly sampled 200 instances from each of four representative datasets, Twitter15, Twitter16, Weibo, and PHEME, and input them into GPT-4o for binary classification (i.e., true or false). As shown in Table III, the performance of GPT-4o on Twitter15 and Twitter16 is limited, with average accuracies of only 37.61% and 38.94%, respectively. The model exhibited considerable inconsistency across the four rumor types, suggesting difficulty in handling category-specific nuances in English social media content. Table IV shows results on the Weibo and PHEME datasets under binary classification. While performance is slightly improved compared to Twitter datasets, average accuracies of 52.15% (Weibo) and 56.32% (PHEME) still reflect suboptimal generalization, especially given the complexity of linguistic and cultural variations present in cross-lingual misinformation. These results highlight that even advanced LLMs lack the task-specific discriminative capacity for robust detection in cross-lingual and culturally nuanced contexts.

Next, we evaluated the upper and lower performance bounds of the proposed method by comparing them with a range of representative baselines across the Twitter15 and Twitter16 datasets. The 7B-parameter base LLM served as the primary subject in all experiments, while the 13B- and 14B-parameter base LLMs, with three augmentation rounds, were introduced to explore the performance upper bound. As shown in Table V, on Twitter15, the Proposed-1 variant achieved an accuracy of 78.11%, surpassing BiGCN (74.52%) and BiMGCL (71.45%) by 3.59% and 6.66%, respectively. Compared to traditional sequential and convolutional models such as LSTM (76.43%), RCNN (73.40%), and Text-CNN (77.45%), Proposed-1 also demonstrated consistent improvements of 1.68%, 4.71%, and 0.66%, respectively. When compared with the attention-based HAN (76.79%) and knowledge-enhanced ELKP (75.70%), Proposed-1 yielded accuracy gains of 1.32% and 2.41%. The performance of the Llama-based variants was even more notable. Proposed-6 achieved an accuracy of 81.81%, outperforming all baselines by a substantial margin: +7.29% over BiGCN, +10.36% over BiMGCL, +5.38% over LSTM, +4.36% over Text-CNN, +8.41% over RCNN, +5.02% over HAN, and +6.11% over ELKP. Proposed-7 and Proposed-8, which use Llama-7B with different training strategies, further verified this trend with accuracies of 78.03% and 80.37%, respectively, while Proposed-9 (based on Llama-13B) achieved the highest performance at 82.34%, exceeding even Proposed-6 by 0.53%. These results demonstrate the effectiveness of our approach and the scalability of LACL across different base model sizes and configurations.

Similarly, as shown in Table VI, on Twitter16, Proposed-1 reached an accuracy of 79.63%, outperforming BiGCN (76.42%) and BiMGCL (75.30%) by 3.21% and 4.33%, respectively. It also surpassed LSTM (75.92%), RCNN (76.54%), Text-CNN (71.45%), HAN (77.16%), and ELKP (77.41%) by 3.71%, 3.09%, 8.18%, 2.47%, and 2.22%, respectively. Among the Llama-based methods, Proposed-6 achieved an accuracy of 84.56%, leading all baseline models with clear margins: +8.14% over BiGCN, +9.26% over BiMGCL, +8.64% over LSTM, +8.02% over RCNN, +7.40% over HAN, +7.15% over ELKP, and +13.11% over Text-CNN. In addition, Proposed-7 and Proposed-8 showed promising performance, reaching 79.91% and 85.08%, respectively. Notably, Proposed-9 obtained the best accuracy of 85.39%, with an Avg F1 of 85.87%, confirming the method's robustness and balanced classification performance across all rumor categories (TR, NR, FR, UR). These results highlight LACL's ability to scale effectively with stronger base LLMs and maintain superior performance across complex misinformation classification tasks.

For the FR category (rumors verified as false or inaccurate), in-depth analysis revealed a consistent performance gap between our proposed method and several baseline models, despite the overall superiority of the proposed variants. On Twitter15, Proposed-1 achieved an F1 score of 75.73%, which was 0.72% lower than BiGCN and 3.75% lower than the best-performing Text-CNN (79.48%), and also fell behind models like HAN and LSTM. Similarly, on Twitter16, BiGCN and BiMGCL surpassed Proposed-1 by 1.97% and 4.06%.

This gap could be attributed to the dual-effect nature of LLM-based data augmentation. While LLMs improved generalization by generating diverse and fluent samples, they were not inherently equipped to verify factual accuracy. During augmentation, LLMs may unintentionally dilute or even rationalize key features indicative of falsehood in FR-class samples. For example, content that originally contained extreme claims, inconsistencies, or manipulative phrasing might have been softened or rephrased, making the misinformation appear more credible. This process likely blurred the semantic boundary between false and true content, thereby undermining the distinctiveness of the FR category.

In the binary classification setting of the Weibo dataset, the proposed method demonstrated clear advantages over all baseline models. As shown in Table VII, Proposed-6 achieved

[1]https://chatgpt.com/

TABLE V
PERFORMANCE COMPARISON (%) ON TWITTER15

Method	ACC	F1				Avg F1
		TR	NR	FR	UR	
BiGCN	74.52	80.07	68.10	76.45	71.04	73.92
BiMGCL	71.45	76.97	66.87	72.99	68.14	71.24
LSTM	76.43	85.20	66.10	75.77	75.34	75.60
Text-CNN	77.45	87.50	68.70	**79.48**	74.19	77.47
RCNN	73.40	80.70	64.46	72.94	72.72	72.71
HAN	76.79	86.22	68.33	76.89	75.70	76.79
ELKP	75.70	73.21	74.66	72.48	75.10	73.86
Proposed-1	78.11	**90.68**	69.42	75.73	74.12	77.48
Proposed-6	**81.81**	89.57	**80.29**	78.43	**78.01**	**81.57**
Proposed-7	78.03	89.52	70.65	76.49	73.18	77.46
Proposed-8	80.37	89.35	78.13	77.82	75.93	80.31
Proposed-9	82.34	88.97	75.78	83.06	80.84	82.16

TABLE VI
PERFORMANCE COMPARISON (%) ON TWITTER16

Method	ACC	F1				Avg F1
		TR	NR	FR	UR	
BiGCN	76.42	86.09	66.68	73.23	75.82	75.45
BiMGCL	75.30	84.79	62.20	75.32	76.36	74.66
LSTM	75.92	90.14	71.11	64.36	81.57	76.80
Text-CNN	71.45	76.97	66.87	72.99	68.14	71.24
RCNN	76.54	90.41	71.26	71.26	77.50	77.06
HAN	77.16	87.17	70.88	70.88	**80.00**	77.20
ELKP	77.41	76.35	74.40	74.40	76.77	75.77
Proposed-1	79.63	94.59	77.64	71.26	76.92	80.10
Proposed-6	84.56	94.59	78.72	76.92	89.74	84.99
Proposed-7	79.91	93.87	78.92	72.13	76.45	80.34
Proposed-8	85.08	95.92	76.89	77.05	85.73	83.90
Proposed-9	85.39	95.45	80.26	79.87	87.89	85.87

TABLE VII
PERFORMANCE COMPARISON (%) ON WEIBO

Method	ACC	F1		Avg F1
		False	True	
LSTM	80.84	80.64	81.02	80.83
Text-CNN	83.87	83.94	83.81	83.88
RCNN	84.23	84.38	83.07	83.73
HAN	82.23	81.30	83.04	82.17
SRD-PSID	83.22	83.09	83.24	83.16
Proposed-1	85.30	87.19	88.41	87.80
Proposed-6	91.63	91.42	91.82	91.62
Proposed-7	86.92	86.58	87.26	86.92
Proposed-8	89.47	89.32	89.61	89.47
Proposed-9	90.78	90.65	90.91	90.78

TABLE VIII
PERFORMANCE COMPARISON (%) ON PHEME

Method	ACC	F1		Avg F1
		False	True	
LSTM	86.89	87.34	86.41	86.88
Text-CNN	85.37	86.08	84.59	85.34
RCNN	87.23	87.48	86.97	87.23
HAN	88.16	88.63	87.65	88.14
ELKP	87.20	87.52	86.08	86.80
Proposed-1	89.01	89.14	88.86	89.00
Proposed-6	91.89	92.21	91.53	91.87
Proposed-7	89.23	88.97	89.48	89.23
Proposed-8	90.87	91.43	90.31	90.87
Proposed-9	91.55	91.98	91.12	91.55

a breakthrough performance with an accuracy of 91.63% and an average F1 score of 91.62%, both exceeding the 90% threshold. Compared to the best-performing baseline in accuracy (RCNN, 84.23%) and in average F1 (Text-CNN, 83.88%), Proposed-6 attained substantial improvements of +7.40% and +7.74%, respectively. Even the lighter Proposed-1 variant, which applied only a single round of LLM-based augmentation, still surpassed all baselines with an accuracy of 85.30% and an average F1 of 87.80%, demonstrating the effectiveness of our augmentation strategy even under low-resource configurations.

On the PHEME dataset, as shown in Table VIII, the proposed models maintained a strong lead, although the margin of improvement was relatively reduced. Proposed-1 achieved 89.01% accuracy and 89.00% average F1, slightly outperforming the best baseline, HAN (88.14%). Proposed-6 continued to lead across all metrics with 91.89% accuracy, 92.21% F1 for False, and 91.53% F1 for True, but the relative performance gap was narrower than that observed on the Weibo dataset.

We also examined the impact of base LLM choice. As shown in Tables V–VIII, when Llama was used as the base model, the corresponding methods (Proposed-7, -8, and -9) consistently demonstrated superior performance across all four datasets. Due to differences in language-specific strengths among base models, Llama outperformed Qwen on the English-based Twitter datasets, while Qwen led on the Chinese-based Weibo dataset. In the fine-tuned setting (Proposed-4 and -8), Qwen consistently yielded slightly better improvements than Llama, suggesting that Qwen offered stronger instruction-following capabilities for the detection task. In the non-fine-tuned configurations (Proposed-1 and -7), the two base models exhibited a trade-off in performance. These results indicated that the proposed method is adaptable to different base LLMs and performs robustly across various model sizes, confirming its versatility and scalability.

These findings indicated that while the proposed method generalized well across datasets, its performance was shaped by the choice of base LLM and parameter scale. In high-context, semantically rich settings like Weibo, Qwen-based models achieved the most notable gains, especially with fine-tuning, whereas Llama-based models excelled on structurally constrained, English-language datasets such as PHEME. Larger LLMs generally delivered higher detection accuracy at the cost of greater computational demands. Overall, the results validated LACL's adaptability to diverse language environments, model sizes, and augmentation strategies, while consistently delivering superior detection performance.

B. Impact of Data Augmentation Rounds

This experiment investigated the impact of data augmentation rounds on model detection performance. As shown in Table IX, the detection accuracy on Twitter15 improved

TABLE IX
RESULTS (%) ON TWITTER15 WITH DIFFERENT AUGMENTATION ROUNDS

Method	ACC	F1				Avg F1
		TR	NR	FR	UR	
Proposed-1	78.11	**90.68**	69.42	75.73	74.12	77.48
Proposed-2	78.45	86.06	**75.55**	75.49	75.52	78.15
Proposed-3	**79.12**	87.89	73.91	79.24	74.28	78.83
Proposed-6	**81.81**	89.57	**80.29**	78.43	78.01	81.57

TABLE X
RESULTS (%) ON TWITTER16 WITH DIFFERENT AUGMENTATION ROUNDS

Method	ACC	F1				Avg F1
		TR	NR	FR	UR	
Proposed-1	79.63	**94.59**	77.64	71.26	76.92	80.10
Proposed-2	80.86	93.33	75	75.86	80.84	81.17
Proposed-3	**83.33**	94.28	76.59	78.16	87.67	84.18
Proposed-6	**84.56**	94.59	78.72	76.92	89.74	84.99

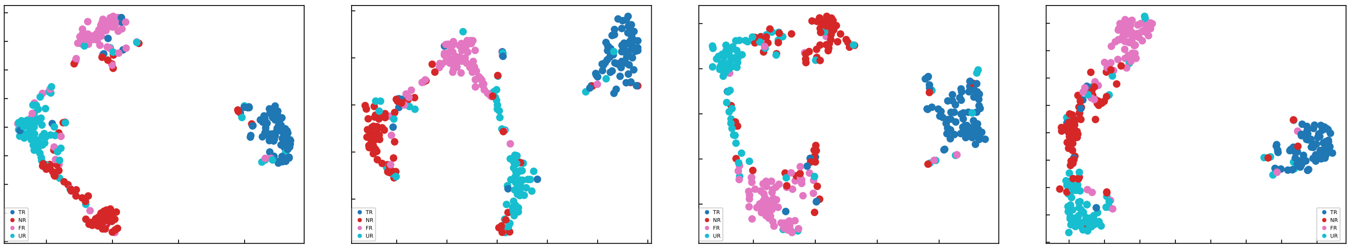

(a) Proposed-1. (b) Proposed-2. (c) Proposed-3. (d) Proposed-6.

Fig. 5. Feature distribution of different augmentation rounds on Twitter15.

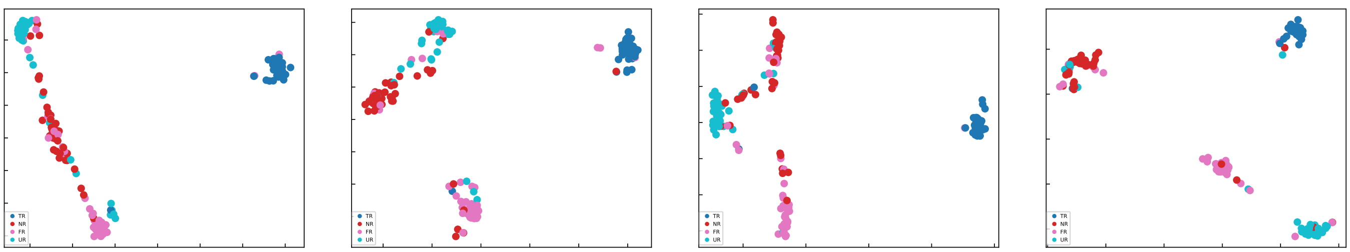

(a) Proposed-1. (b) Proposed-2. (c) Proposed-3. (c) Proposed-6.

Fig. 6. Feature distribution of different augmentation rounds on Twitter16.

gradually with additional augmentation rounds. Specifically, Proposed-3 achieved a 0.67% and 1.01% accuracy increase compared to Proposed-1 and -2, respectively. Similarly, as presented in Table X for Twitter16, Proposed-3 improved accuracy by 2.47% and 3.7% compared to Proposed-1 and -2, although it fell short of Proposed-6, which achieved the highest accuracy of 84.56%. Feature visualizations further illustrated that increased augmentation rounds made class boundaries more distinct. This phenomenon could be attributed to two factors. First, as the number of augmentation rounds increased, the generated data samples became more diverse, allowing the model to learn more comprehensive features. On the other hand, larger parameter LLMs, with their superior language and contextual understanding, generated higher-quality samples, thereby enhancing detection performance.

However, category-specific detection results exhibited noticeable fluctuations. On Twitter15, Proposed-1 achieved the best performance for the *TR* (True Rumor) category. As shown in Figs. 5(a) and 5(b), the TR feature points of Proposed-1 were more tightly clustered than those of Proposed-2, indicating more stable class separation. For the *NR* (Non-Rumor) category, Proposed-2 outperformed Proposed-3, as illustrated in Figs. 5(b) and 5(c), yet both remained inferior to Proposed-6, which exhibited better inter-class separation. Notably, Fig.5(c) revealed significant overlap between NR and *UR* (Unverified Rumor) feature points in Proposed-3, reflecting ambiguity in feature space. Similar trends were observed on Twitter16 in Figs. 6(a)–(d), where Proposed-6 consistently showed stronger feature discrimination across categories.

These fluctuations stem mainly from variations in LLM-augmented data quality across categories and the occasional introduction of features misaligned with original class semantics. Although augmentation improved overall performance, its effect on fine-grained category boundaries remained sensitive to data quality and semantic consistency.

As shown in Table XI, increasing the LLM augmentation rounds from 1 to 3 improved classification accuracy on Weibo from 87.88% to 89.70%, narrowing the F1-score gap between True and False classes from 0.91% to 0.36%. Feature visualizations (Fig. 7) illustrated that False-class samples transitioned from a bimodal (Proposed-1) to an unimodal distribution (Proposed-2), with decreased overlap between classes. Although Proposed-3 improved clustering compactness, the True class consistently retained a bimodal distribution. On PHEME (Table XII), accuracy improved from 89.01% to 90.61% across augmentation rounds. True and False class F1-scores increased to 90.20% and 90.99%, respectively. Feature distributions (Fig. 8) revealed similar clustering enhancements, shifting the False class from bimodal to unimodal distribution, and reducing inter-class overlap. However, the True class again

TABLE XI
RESULTS (%) ON WEIBO WITH DIFFERENT AUGMENTATION ROUNDS

Method	ACC	F1		Avg
		False	True	F1
Proposed-1	87.88	87.40	88.31	87.86
Proposed-2	88.62	88.30	88.93	88.62
Proposed-3	89.70	89.51	89.87	89.69
Proposed-6	**91.63**	91.42	91.82	91.62

TABLE XII
RESULTS (%) ON PHEME WITH DIFFERENT AUGMENTATION ROUNDS

Method	ACC	F1		Avg
		False	True	F1
Proposed-1	89.01	89.14	88.86	89.00
Proposed-2	89.94	90.21	89.66	89.94
Proposed-3	90.61	90.99	90.20	90.60
Proposed-6	**91.89**	92.21	91.53	91.87

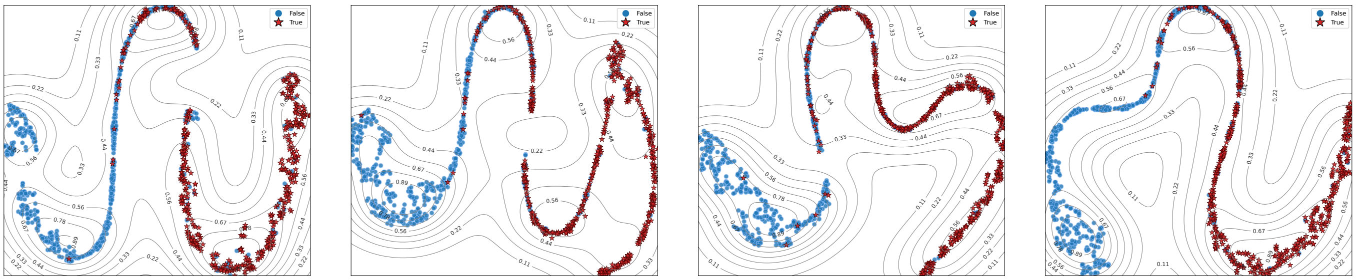

(a) Proposed-1. (b) Proposed-2. (c) Proposed-3. (d) Proposed-6.

Fig. 7. Feature distribution of different augmentation rounds on Weibo.

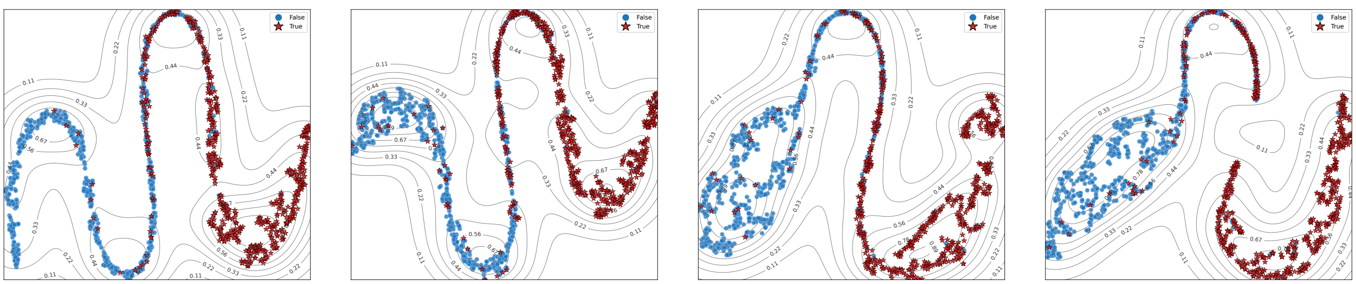

(a) Proposed-1. (b) Proposed-2. (c) Proposed-3. (c) Proposed-6.

Fig. 8. Feature distribution of different augmentation rounds on PHEME.

maintained its bimodal feature distribution.

Overall, two conclusions could be drawn: 1) increased augmentation rounds enhanced sample diversity, aiding comprehensive feature learning; 2) larger LLMs produced higher-quality augmented samples, though larger parameter scales implied higher training and fine-tuning costs.

C. Impact of LLM Fine-Tuning Rounds

The experimental results above confirmed that the proposed LACL was highly adaptable to different base LLMs. In this subsection, we took Qwen-based configurations (Proposed-3, -4, -5, and -6) as the research objects and investigated the influence of fine-tuning rounds on detection performance.

As the number of fine-tuning rounds for Qwen-7B increased, LLM-assisted CL detection accuracy improved, though it did not surpass the performance of Proposed-6. Specifically, on Twitter15, as shown in Table XIII, F1 scores for the *NR* and *FR* categories fluctuated significantly. Compared to Proposed-3, Proposed-4 saw a 7.27% decrease in the *NR* F1 score but a 7.57% increase in the *FR* F1 score. Other categories generally showed an upward trend in F1 scores. Fig. 9 clarified these results: initially, the *NR* and *FR* categories overlapped significantly, which lowered the accuracy for *FR*. After two fine-tuning rounds, *FR* showed stronger clustering and more compact feature distribution, while *NR* experienced weaker clustering and increased overlap with the UR category.

On Twitter16, as shown in Table XIV, the F1 scores for *TR* and *NR* categories steadily improved. For the *FR* category, Proposed-4 and -5 achieved F1 scores 1.88% and 1% lower than Proposed-3, respectively. Similarly, in the *UR* category, Proposed-4 and -5 exhibited decreases of 1.56% and 0.83% compared to Proposed-3. Fig. 10 illustrated that the clustering degree of feature points increased with the number of fine-tuning rounds; however, overlaps for *FR*, *UR*, and *NR* categories negatively impacted detection precision. This underscored the model's progressive optimization in feature extraction. The recognition of natural samples improved with iterations, yielding cumulative F1 score gains of 1.63% for *TR* and 1.7% for *NR*. Additionally, classification ambiguity persisted for boundary samples, particularly in overlapping regions of *FR* and *UR* categories, leading to slight performance degradation. F1 scores remained within a narrow range of 84–85%, while *UR* metrics displayed an initial decline followed by a recovery.

As shown in Table XV, increasing the number of LLM fine-tuning rounds (from Proposed-3 to -4 to -5) led to

TABLE XIII
RESULTS (%) ON TWITTER15 WITH DIFFERENT FINE-TUNING TIMES

Method	ACC	F1				Avg
		TR	NR	FR	UR	F1
Proposed-3	79.12	87.89	73.91	79.24	74.28	78.83
Proposed-4	80.13	88.88	**79.10**	76.64	75.71	80.08
Proposed-5	80.81	89.87	**71.83**	**84.21**	77.63	80.89
Proposed-6	81.81	89.57	80.29	78.43	78.01	81.58

TABLE XIV
RESULTS (%) ON TWITTER16 WITH DIFFERENT FINE-TUNING TIMES

Method	ACC	F1				Avg
		TR	NR	FR	UR	F1
Proposed-3	83.33	94.28	76.59	**78.16**	**87.67**	84.18
Proposed-4	85.24	95.89	77.53	76.28	86.11	83.95
Proposed-5	85.31	95.91	78.29	**77.16**	**86.84**	85.55
Proposed-6	**84.56**	94.59	78.72	76.92	89.74	84.99

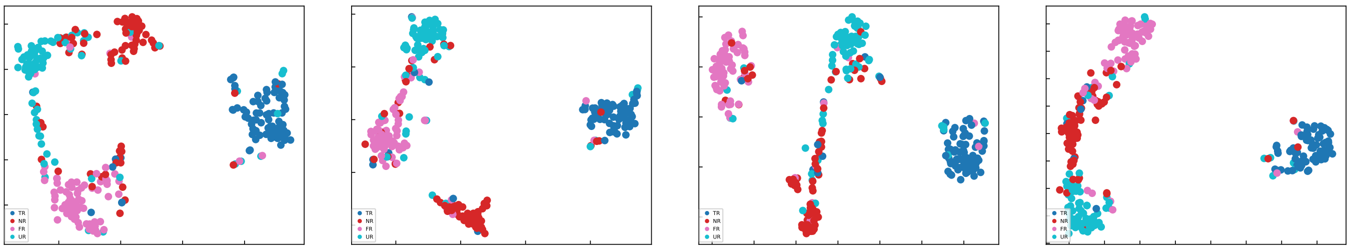

(a) Proposed-3. (b) Proposed-4. (c) Proposed-5. (d) Proposed-6.

Fig. 9. Feature distribution of different fine-tuning rounds on Twitter15.

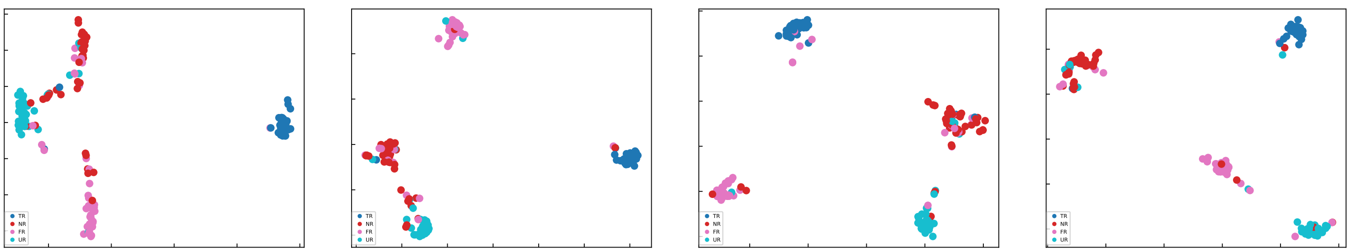

(a) Proposed-3. (b) Proposed-4. (c) Proposed-5. (d) Proposed-6.

Fig. 10. Feature distribution of different fine-tuning rounds on Twitter16.

consistent performance improvements on the Weibo dataset. Specifically, accuracy rose from 89.70% to 90.45%, while the F1-scores for the True and False classes increased to 90.41% and 90.14%, respectively, indicating enhanced class balance. Feature distribution visualizations in Fig. 11(a) revealed overlapping density contours (e.g., 0.56) between classes and a bimodal distribution in the True class. With one round of fine-tuning (Fig. 11(b)), this bimodality persisted in the core region (0.78–0.89). However, after two rounds (Fig. 11(c)), feature points became more concentrated in the lower-right quadrant, suggesting that fine-tuning refined LLM parameters and promoted tighter intra-class clustering in the feature space.

Similarly, on the PHEME dataset (Table XVI), fine-tuning (Proposed-4 and -5) resulted in steady performance gains: accuracy improved from 90.61% to 91.29%, and the True/False class F1-scores increased from 90.20%/90.99% to 90.96%/91.61%. Visualization in Fig. 12 showed that transitioning from no fine-tuning (Proposed-3) to one round (Proposed-4) reduced class overlap in the central region. Further, Fig. 12(b) and (c) demonstrated that Proposed-5 yielded more compact True-class clusters and sparser density contours in overlapping regions. Notably, despite these improvements, the 14B-based Proposed-6 model still outperformed both Proposed-4 and -5 across all metrics on both datasets.

D. *Resource Occupancy Analysis in Offline Training*

In this experiment, models of different scales exhibited varying resource consumption during data augmentation and fine-tuning processes. For the data augmentation task (Table XVII), both Qwen-7B and Llama-7B used dual 4090 GPUs with data parallelism, while larger models, Qwen-14B and Llama-13B, employed model parallelism.

Data Parallelism involves splitting the data into smaller batches, which are distributed across multiple GPUs. Each GPU processes a subset of the data, and the gradients are averaged across the GPUs during training. This technique is efficient when the model can fit within the memory of a single GPU but requires multiple GPUs to handle larger batches. On the other hand, Model Parallelism divides the model itself across multiple GPUs. Each GPU stores and processes a portion of the model, allowing for the training of much larger models that exceed the memory capacity of a single GPU. This method is useful for models with large numbers of parameters but comes with higher inter-GPU communication overhead.

The latter models, which require model parallelism, have a significantly higher memory footprint compared to the former models using data parallelism. In the model fine-tuning phase (Table XVIII), both Qwen-7B and Llama-7B again utilized dual 4090 GPUs, but the display memory consumption further

This article has been accepted for publication in IEEE Transactions on Computational Social Systems. This is the author's version which has not been fully edited and content may change prior to final publication. Citation information: DOI 10.1109/TCSS.2025.3599080

TABLE XV
RESULTS (%) ON WEIBO WITH DIFFERENT FINE-TUNING TIMES

Method	ACC	F1		Avg F1
		False	True	
Proposed-3	89.70	89.51	89.51	89.69
Proposed-4	90.23	90.05	90.41	90.23
Proposed-5	90.45	90.14	90.41	90.33
Proposed-6	91.63	91.42	91.82	91.62

TABLE XVI
RESULTS (%) ON PHEME WITH DIFFERENT FINE-TUNING TIMES

Method	ACC	F1		Avg F1
		False	True	
Proposed-3	90.61	90.99	90.20	90.59
Proposed-4	91.04	91.26	90.79	91.02
Proposed-5	91.29	91.61	90.96	91.28
Proposed-6	91.89	92.21	91.53	91.87

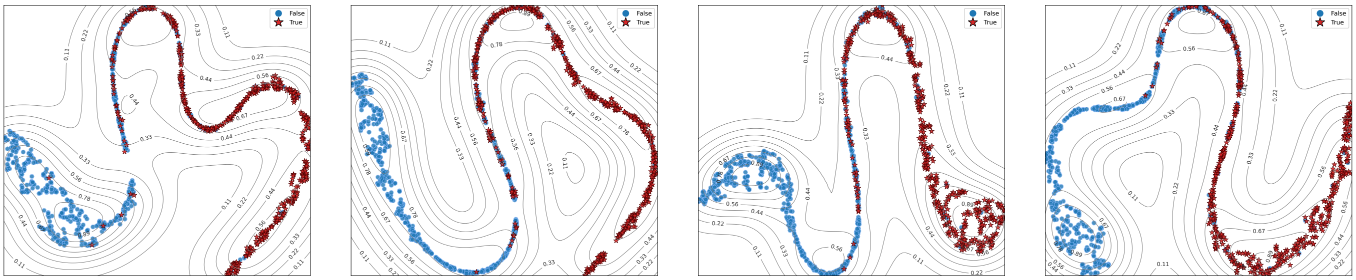

(a) Proposed-3. (b) Proposed-4. (c) Proposed-5. (d) Proposed-6.

Fig. 11. Feature distribution of different fine-tuning rounds on Weibo.

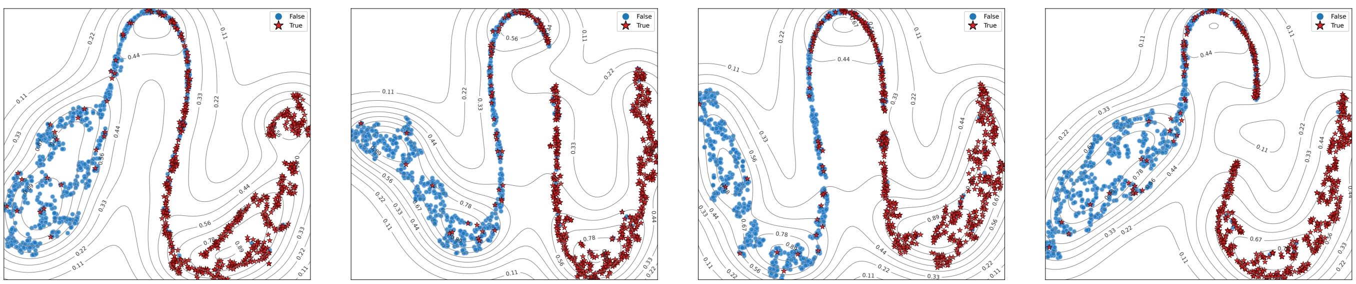

(a) Proposed-3. (b) Proposed-4. (c) Proposed-5. (d) Proposed-6.

Fig. 12. Feature distribution of different fine-tuning rounds on PHEME.

TABLE XVII
MEMORY USAGE AND INFERENCE MODE IN LLM DATA AUGMENTATION

Method(s)	Base LLM	GPU	Avg Mem Usage	Inference Mode
Proposed-1 to -5	Qwen-7B	Dual RTX 4090	14.4 GB per card	Data Parallelism
Proposed-6	Qwen-14B	Dual RTX 4090	22.6 GB per card	Model Parallelism
Proposed-7 and -8	Llama-7B	Dual RTX 4090	14.6 GB per card	Data Parallelism
Proposed-9	Llama-13B	Dual RTX 4090	21.1 GB per card	Model Parallelism

TABLE XVIII
GPU DEVICES AND MEMORY USAGE IN LLM FINE-TUNING

Method(s)	Base LLM	GPU	Avg Mem Usage
Proposed-4 Proposed-5	Qwen-7B	Dual RTX 4090	20.9 GB per card
Proposed-8	Llama-7B	Dual RTX 4090	21.8 GB per card

increased, highlighting the substantial rise in display memory demand during fine-tuning. These results demonstrated that as model size and complexity increased, memory usage grew, with larger models requiring model parallelism for efficient inference, significantly increasing GPU memory consumption compared to smaller models using data parallelism.

V. CONCLUSION

This study introduces LACL, a novel framework that integrates LLMs with CL to advance misinformation detection in social networks. The innovation lies in leveraging contrastive loss-guided LLM fine-tuning for data augmentation, which generates semantically rich, diverse, and consistent samples to address challenges such as limited labeled data and complex semantics. By establishing a feedback loop between the LLM and CL, LACL progressively enhances both augmentation quality and feature extraction capability. Extensive experiments on four benchmark datasets demonstrate that LACL outperforms conventional CL-based methods and direct, task-unadapted LLM applications, achieving notable gains in detection accuracy and F1-score, especially in high-context environments like Weibo. The results further confirm that fine-tuned LLMs consistently surpass non-fine-tuned counterparts, and that LACL maintains robust performance across different base LLMs and model scales, underscoring its adaptability and scalability for diverse detection scenarios.

The proposed framework is inherently extensible and, with domain-specific customization, can be applied to other high-stakes detection tasks such as cybersecurity threat detection and medical filtering. Future work will focus on extending LACL to cross-lingual and multimodal settings, while exploring real-time adaptation and hallucination mitigation strategies to enhance robustness and applicability.

REFERENCES

[1] S. A. Aljawarneh and S. A. Swedat, "Fake news detection using enhanced BERT," *IEEE Transactions on Computational Social Systems*, vol. 11, no. 4, pp. 4843–4850, 2024.

[2] M.-Y. Chen, Y.-W. Lai, and J.-W. Lian, "Using deep learning models to detect fake news about COVID-19," *ACM Transactions on Internet Technology*, vol. 23, no. 2, pp. 1–23, 2023.

[3] Y. Liu and Y.-F. B. Wu, "FNED: A deep network for fake news early detection on social media," *ACM Transactions on Information Systems*, vol. 38, no. 3, pp. 1–33, 2020.

[4] S. Dutta, S. Caur, S. Chakrabarti, and T. Chakraborty, "Semi-supervised stance detection of tweets via distant network supervision," in *Proc. of the ACM International Conference on Web Search and Data Mining*, 2022, p. 241–251.

[5] P. Meel and D. K. Vishwakarma, "A temporal ensembling based semi-supervised convnet for the detection of fake news articles," *Expert Systems with Applications*, vol. 177, p. 115002, 2021.

[6] J. Mukhoti, T.-Y. Lin, O. Poursaeed, R. Wang, A. Shah, P. H. Torr, and S.-N. Lim, "Open vocabulary semantic segmentation with patch aligned contrastive learning," in *Proc. of the IEEE/CVF Conference on Computer Vision and Pattern Recognition*, 2023, pp. 19 413–19 423.

[7] Y. Liu, L. Huang, F. Giunchiglia, X. Feng, and R. Guan, "Improved graph contrastive learning for short text classification," in *Proc. of the AAAI Conference on Artificial Intelligence*, vol. 38, no. 17, 2024, pp. 18 716–18 724.

[8] S. Zhao, C. Wang, M. Hu, T. Yan, and M. Wang, "MCL: Multi-granularity contrastive learning framework for chinese ner," in *Proc. of the AAAI Conference on Artificial Intelligence*, vol. 37, no. 11, 2023, pp. 14 011–14 019.

[9] S. Li, W. Li, A. M. Luvembe, and W. Tong, "Graph contrastive learning with feature augmentation for rumor detection," *IEEE Transactions on Computational Social Systems*, vol. 11, no. 4, pp. 5158–5167, 2024.

[10] Y. Jiang, C. Huang, and L. Huang, "Adaptive graph contrastive learning for recommendation," in *Proc. of the 29th ACM SIGKDD Conference on Knowledge Discovery and Data Mining*, 2023, pp. 4252–4261.

[11] A. Giachanou, P. Rosso, and F. Crestani, "The impact of emotional signals on credibility assessment," *Journal of the Association for Information Science and Technology*, vol. 72, no. 9, pp. 1117–1132, 2021.

[12] Y. Rong, W. Huang, T. Xu, and J. Huang, "DropEdge: Towards deep graph convolutional networks on node classification," in *Proc. of International Conference on Learning Representations*, 2020, pp. 1–17.

[13] D. Chen, Y. Lin, W. Li, P. Li, J. Zhou, and X. Sun, "Measuring and relieving the over-smoothing problem for graph neural networks from the topological view," in *Proc. of the AAAI Conference on Artificial Intelligence*, vol. 34, no. 04, 2020, pp. 3438–3445.

[14] Y. Wang, W. Wang, Y. Liang, Y. Cai, J. Liu, and B. Hooi, "NodeAug: Semi-supervised node classification with data augmentation," in *Proc. of the 26th ACM SIGKDD International Conference on Knowledge Discovery and Data Mining*, 2020, pp. 207–217.

[15] J. Wei and K. Zou, "EDA: Easy data augmentation techniques for boosting performance on text classification tasks," *arXiv preprint arXiv:1901.11196*, 2019.

[16] A. Zhong, D. Mo, G. Liu, J. Liu, Q. Lu, Q. Zhou, J. Wu, Q. Li, and Q. Wen, "Logparser-LLM: Advancing efficient log parsing with large language models," in *Proc. of the 30th ACM SIGKDD Conference on Knowledge Discovery and Data Mining*, 2024, p. 4559–4570.

[17] F. Li, H. Shen, J. Mai, T. Wang, Y. Dai, and X. Miao, "Pre-trained language model-enhanced conditional generative adversarial networks for intrusion detection," *Peer-to-Peer Networking and Applications*, vol. 17, no. 1, pp. 227–245, 2024.

[18] J. Yang, X. Wang, Y. Zhao, Y. Liu, and F.-Y. Wang, "RAG-based crowdsourcing task decomposition via masked contrastive learning with prompts," *IEEE Transactions on Computational Social Systems*, vol. 12, no. 4, pp. 1535–1547, 2025.

[19] L. Huang, W. Yu, W. Ma, W. Zhong, Z. Feng, H. Wang, Q. Chen, W. Peng, X. Feng, B. Qin, and T. Liu, "A survey on hallucination in large language models: Principles, taxonomy, challenges, and open questions," *ACM Transactions on Information Systems*, vol. 43, no. 2, 2024.

[20] W. Feng, Y. Li, B. Li, Z. Jia, and Z. Chu, "BiMGCL: rumor detection via bi-directional multi-level graph contrastive learning," *PeerJ Computer Science*, vol. 9, p. e1659, 2023.

[21] J. Wu, J. Guo, and B. Hooi, "Fake news in sheep's clothing: Robust fake news detection against LLM-empowered style attacks," in *Proc. of the 30th ACM SIGKDD Conference on Knowledge Discovery and Data Mining*, 2024, p. 3367–3378.

[22] F. Liu, X. Zhang, and Q. Liu, "An emotion-aware approach for fake news detection," *IEEE Transactions on Computational Social Systems*, vol. 11, no. 3, pp. 3516–3524, 2024.

[23] D. Saxena and J. Cao, "Generative adversarial networks (GANs) challenges, solutions, and future directions," *ACM Computing Surveys*, vol. 54, no. 3, pp. 1–42, 2021.

[24] B. Hu, Q. Sheng, J. Cao, Y. Shi, Y. Li, D. Wang, and P. Qi, "Bad actor, good advisor: Exploring the role of large language models in fake news detection," in *Proc. of the AAAI Conference on Artificial Intelligence*, vol. 38, no. 20, 2024, pp. 22 105–22 113.

[25] Y. Li, X. Zhai, M. Alzantot, K. Yu, I. Vulić, A. Korhonen, and M. Hammad, "CALRec: Contrastive alignment of generative LLMs for sequential recommendation," in *Proc. of the 18th ACM Conference on Recommender Systems*, 2024, p. 422–432.

[26] Q. Dong, Y. Liu, Q. Ai, Z. Wu, H. Li, Y. Liu, S. Wang, D. Yin, and S. Ma, "Unsupervised large language model alignment for information retrieval via contrastive feedback," in *Proc. of the 47th International ACM SIGIR Conference on Research and Development in Information Retrieval*, 2024, p. 48–58.

[27] C. Jiang, H. Xu, M. Dong, J. Chen, W. Ye, M. Yan, Q. Ye, J. Zhang, F. Huang, and S. Zhang, "Hallucination augmented contrastive learning for multimodal large language model," in *Proc. of the IEEE/CVF Conference on Computer Vision and Pattern Recognition*, 2024, pp. 27 036–27 046.

[28] B. Chen and A. L. Bertozzi, "AutoKG: Efficient automated knowledge graph generation for language models," in *Proc. of IEEE International Conference on Big Data*, 2023, pp. 3117–3126.

[29] B. Xie, X. Ma, X. Shan, A. Beheshti, J. Yang, H. Fan, and J. Wu, "Multiknowledge and llm-inspired heterogeneous graph neural network for fake news detection," *IEEE Transactions on Computational Social Systems*, vol. 12, no. 2, pp. 682–694, 2025.

[30] G. Jawahar, B. Sagot, and D. Seddah, "What does BERT learn about the structure of language?" in *Proc. of the 57th Annual Meeting of the Association for Computational Linguistics*, 2019, pp. 3651–3657.

[31] M.-C. Popescu, V. E. Balas, L. Perescu-Popescu, and N. Mastorakis, "Multilayer perceptron and neural networks," *WSEAS Transactions on Circuits and Systems*, vol. 8, no. 7, pp. 579–588, 2009.

[32] R. Hadsell, S. Chopra, and Y. LeCun, "Dimensionality reduction by learning an invariant mapping," in *Proc. of the IEEE/CVF Conference on Computer Vision and Pattern Recognition*, vol. 2, 2006, pp. 1735–1742.

[33] K. Lv, Y. Yang, T. Liu, Q. Gao, Q. Guo, and X. Qiu, "Full parameter fine-tuning for large language models with limited resources," *arXiv preprint arXiv:2306.09782*, 2023.

[34] Y. Gu, X. Han, Z. Liu, and M. Huang, "PPT: Pre-trained prompt tuning for few-shot learning," in *Proc. of the 60th Annual Meeting of the Association for Computational Linguistics*, 2022, pp. 8410–8423.

[35] N. Ding, Y. Qin, G. Yang, F. Wei, Z. Yang, Y. Su, S. Hu, Y. Chen, C.-M. Chan, W. Chen *et al.*, "Parameter-efficient fine-tuning of large-scale pre-trained language models," *Nature Machine Intelligence*, vol. 5, no. 3, pp. 220–235, 2023.

[36] E. J. Hu, Y. Shen, P. Wallis, Z. Allen-Zhu, Y. Li, S. Wang, L. Wang, and W. Chen, "LoRA: Low-rank adaptation of large language models," *arXiv preprint arXiv:2106.09685*, 2021.

[37] K. He, H. Fan, Y. Wu, S. Xie, and R. Girshick, "Momentum contrast for unsupervised visual representation learning," in *Proc. of the IEEE/CVF Conference on Computer Vision and Pattern Recognition*, 2020, pp. 9729–9738.

[38] J. Ma, W. Gao, and K.-F. Wong, "Detect rumors in microblog posts using propagation structure via kernel learning," in *Proc. of the 55th Annual Meeting of the Association for Computational Linguistics*, 2017, pp. 708–717.

[39] C. Yuan, Q. Ma, W. Zhou, J. Han, and S. Hu, "Jointly embedding the local and global relations of heterogeneous graph for rumor detection," in *Proc. of IEEE International Conference on Data Mining (ICDM)*, 2019, pp. 796–805.
[40] E. Kochkina, M. Liakata, and A. Zubiaga, "All-in-one: Multi-task learning for rumour verification," in *Proc. of the 27th International Conference on Computational Linguistics*, 2018, pp. 3402–3413.
[41] T. Bian, X. Xiao, T. Xu, P. Zhao, W. Huang, Y. Rong, and J. Huang, "Rumor detection on social media with bi-directional graph convolutional networks," in *Proc. of the AAAI Conference on Artificial Intelligence*, vol. 34, no. 01, 2020, pp. 549–556.
[42] H. Aydın, Z. Orman, and M. A. Aydın, "A long short-term memory (LSTM)-based distributed denial of service (DDoS) detection and defense system design in public cloud network environment," *Computers & Security*, vol. 118, p. 102725, 2022.
[43] Y. Kim, "Convolutional neural networks for sentence classification," in *Proc. of the Conference on Empirical Methods in Natural Language Processing (EMNLP)*, 2014, pp. 1746–1751.
[44] R. Girshick, J. Donahue, T. Darrell, and J. Malik, "Rich feature hierarchies for accurate object detection and semantic segmentation," in *Proc. of the IEEE Conference on Computer Vision and Pattern Recognition*, 2014, pp. 580–587.
[45] Z. Yang, D. Yang, C. Dyer, X. He, A. Smola, and E. Hovy, "Hierarchical attention networks for document classification," in *Proc. of the Conference of the North American Chapter of the Association for Computational Linguistics: Human Language Technologies*, 2016, pp. 1480–1489.
[46] Y. Yan, P. Zheng, and Y. Wang, "Enhancing large language model capabilities for rumor detection with knowledge-powered prompting," *Engineering Applications of Artificial Intelligence*, vol. 133, p. 108259, 2024.
[47] Y. Gao, X. Wang, X. He, H. Feng, and Y. Zhang, "Rumor detection with self-supervised learning on texts and social graph," *Frontiers of Computer Science*, vol. 17, no. 4, p. 174611, 2023.
[48] J. Bai, S. Bai, Y. Chu, Z. Cui, K. Dang, X. Deng, Y. Fan, W. Ge, Y. Han, F. Huang *et al.*, "Qwen technical report," *arXiv preprint arXiv:2309.16609*, 2023.
[49] H. Touvron, T. Lavril, G. Izacard, X. Martinet, M.-A. Lachaux, T. Lacroix, B. Rozière, N. Goyal, E. Hambro, F. Azhar *et al.*, "Llama: Open and efficient foundation language models," *arXiv preprint arXiv:2302.13971*, 2023.

Hang Shen (Member, IEEE) received the Ph.D. degree with honors in Computer Science from the Nanjing University of Science and Technology, Nanjing, China, in 2015. He worked as a Full-Time Postdoctoral Fellow with the Broadband Communications Research (BBCR) Lab, Electrical and Computer Engineering Department, University of Waterloo, Waterloo, ON, Canada, from 2018 to 2019. He is currently an Associate Professor with the Department of Computer Science and Technology at Nanjing Tech University, Nanjing, China. His research interests involve wireless networking and cybersecurity. He serves as an Associate Editor for *Journal of Information Processing Systems*, *Frontiers in Blockchain*, and IEEE ACCESS, and was a Guest Editor for *Peer-to-Peer Networking and Applications*. He is/was a Program Committee Member of the IEEE International Conference on High Performance Computing and Communications (HPCC), the International Conference on Algorithms and Architectures for Parallel Processing (ICA3PP), the Annual International Conference on Privacy, Security and Trust (PST), and the International Conference on Artificial Intelligence Computing and Systems (AICompS). He is an IEEE member, an Executive Committee Member of the ACM Nanjing Chapter, and a Supervisory Committee Member of the CCF Nanjing Chapter.

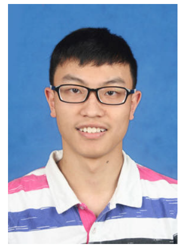

Xiang Li received the B.Eng. degree in Network Engineering from Nanjing Institute of Technology, Nanjing, China. He is currently pursuing the M.Eng. degree in Computer Science at Nanjing Tech University, Nanjing, China. His research interests include large language models and knowledge graphs for cybersecurity. He is a CCF student member.

Xu Wang received the B.Sc. degree in Information and Computational Science, and M.Eng. degree in Computer Science, both from Nanjing Tech University, Nanjing, China. His research interests include unsupervised and semi-supervised learning, as well as large language models for cybersecurity.

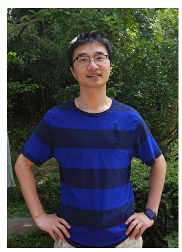

Yuanfei Dai received the Ph.D. degree in Computer Science from Fuzhou University, Fuzhou, China, in 2021. From 2019 to 2020, he was a Visiting Student at Brown University, Providence, RI, USA. He is currently a Lecturer at Nanjing Tech University, Nanjing, China. His research interests include knowledge acquisition and knowledge graph representation. He, together with his student, received the Best Student Paper Award at the 2023 International Conference on Knowledge Science, Engineering and Management (KSEM).

Tianjing Wang (Member, IEEE) holds a B.Sc. in Mathematics from Nanjing Normal University in 2000, an M.Sc. in Mathematics from Nanjing University in 2002, and a Ph.D. in Signal and Information System from the Nanjing University of Posts and Telecommunications (NUPT) in 2009, all in Nanjing, China. From 2011 to 2013, she was a Full-Time Postdoctoral Fellow with the School of Electronic Science and Engineering at NUPT. From 2013 to 2014, she served as a Visiting Scholar in the Electrical and Computer Engineering Department at the State University of New York at Stony Brook. She is an Associate Professor at Nanjing Tech University. Her research interests include cybersecurity and vehicular networks. She is a member of IEEE and CCF.

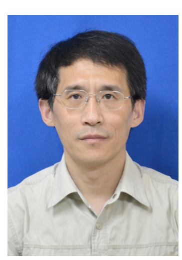

Guangwei Bai received the B.Eng. and M.Eng. degrees in computer engineering from Xi'an Jiaotong University, Xi'an, China, in 1983 and 1986, respectively, and the Ph.D. degree in Computer Science from the University of Hamburg, Hamburg, Germany, in 1999. From 1999 to 2001, he worked as a Research Scientist at the German National Research Center for Information Technology, Germany. In 2001, he joined the University of Calgary, Calgary, AB, Canada, as a Research Associate. Since 2005, he has been working at Nanjing Tech University, Nanjing, China, as a Professor in Computer Science. From October to December 2010, he was a visiting professor in the Electrical and Computer Engineering Department at the University of Waterloo, Waterloo, ON, Canada. His research interests include wireless networking and cybersecurity.